Presented at the 19th Annual CMAS Conference, Chapel Hill, NC, October 26-28, 2020

REMOTE SENSING-BASED ESTIMATES OF WASTES BURNING IN TEHRAN, IRAN

Farzaneh Taksibi, Hossein Khajehpour* , Yadollah Saboohi
Energy Engineering Department, Sharif University of Technology, Tehran, Iran

1. INTRODUCTION

Policymakers use emission inventory from different sources to determine significant sources of air pollutants and to target controlling actions.

The VIIRS Night fire products can detect thermal anomalies to study the spatial and temporal changes built on the well-established VIIRS fire and thermal anomalies product. In this method, many emission sources that were unknown to policymakers will be identified. One of the main unidentified sources is emissions from the crop residue burning and agricultural wastes which adversely affect the regional air quality and public health.

The purpose of this study is to provide a remote sensing methodology for the identification of the time and place of thermal anomalies around Tehran with the help of VIIRS night fire products. This gives an estimation of the temperatures of sub-pixel heat sources, to evaluate the spatiotemporal pattern of uncontrolled burning.

In this case, thermal anomalies around Tehran have been observed from 2017 to 2019 and their impact on monitoring stations based on meteorological conditions with the help of the Hysplit model has been evaluated. By comparing the effects of the non-systematic emission sources on nearby monitoring stations, the contribution of the anomalies on Tehran's air quality is investigated.

Tehran, the capital of Iran, has been among the most polluted Megacities in the world (Martin and Maria 2018). Based on available data from the monitoring stations from March 2019 to March 2020, the Air Quality Index of only 8% of the days were categorized as clean days (TAQCC 2020). $PM_{2.5}$ has been the criteria pollutant in Tehran in recent years (TAQCC 2020). The $PM_{2.5}$ emission inventory which is reported by Tehran Air Quality Control Company (TAQCC) indicates that 60.8 % of total primary $PM_{2.5}$ emissions are originated from mobile sources and 39.2% is from stationary resources including industries, power plants, oil refinery and residential sectors (Shahidzadeh 2019). There are no statistics on agricultural emissions in the reported Tehran emission inventory. However, other studies in Tehran's emission inventory show that the agricultural sector in Tehran may contribute to 0.6 kt of $PM_{2.5}$ emissions; which is 5.7 percent of the total emissions (Taksibi et al. 2020).

Tehran is surrounded by 44,858 hectares of agricultural land from south to west. In this area, agricultural residue burning is commonly practiced primarily to manage the remaining agricultural wastes after harvesting and for preparing the field for the next cropping cycle in a short time. Moreover, there is a municipal waste center near Tehran which may burn a small share of wastes every year. Figure 1 shows Tehran and surrounding agricultural lands around this city.

Figure 1 Tehran location

2. METHODOLOGY

In this study Identification of the time and place of thermal anomalies with the help of VIIRS night fire products in *the world view map* from 2017 to

*Corresponding author: Hossein Khajehpour,
Energy Engineering Department,
Sharif University of Technology, Tehran, Iran;
e-mail: khajehpour@energy.sharif.edu

2019 has been implemented and the anomalies caused by the agricultural sector and waste management has recognized by Landsat 8 satellite products. Moreover, based on the meteorological conditions and topographic specifications, the trajectory of emissions in these points is investigated with the help of the Hysplite model.
Considering air pollution monitoring stations, the effect of the crop and waste burning emissions on the air quality of the city may be evaluated. Figure 2 indicates this process.

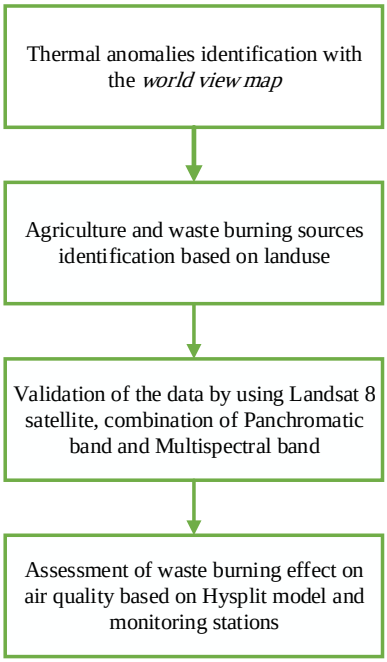

Figure 2 methodology for agricultural waste burnings identification

2.1 Thermal anomalies identification

The Visible Infrared Imaging Radiometer Suite (VIIRS) sensor on the Suomi National Polar-orbiting Partnership (S-NPP) satellite incorporates fire-sensitive channels (Csiszar et al. 2014). VIIRS has a swath of 3,040 km and provides full global coverage. The 375 m datasets are highly used in fire management and other research purposes due to higher spatial resolution, which allows it to detect a greater number of fires even of small intensity (Singh et al. 2020). Suomi NPP satellite passes through 1:30 pm, and 1:30 am local time and has a fire band with a spatial resolution of 375 m (VIIRS 2020).

The World View Map visually explores the past and the present from a satellite's perspective view and provides a spatiotemporal pattern of heat-releasing of thermal anomalies produced by The MODIS and the VIIRS products (WORLDVIEW 2020).

1.1. Landsat 8

Landsat 8 carries OLI and TIR sensors. OLI generates 9 spectral bands (Band 1 to 9) which consist of coastal, blue, green, red, NIR, SWIR-1, SWIR-2, and cirrus. These 8 bands have a ground resolution of 30 meters. The panchromatic band has a finer resolution of 15 meters(Vermote et al. 2016). The Thermal Infrared Sensor (TIRS) is centered at roughly 10.9 and 12 am (Bands 10 and 11 respectively). They have 100 m spatial resolution and can observed land surface temperature (Jiménez-Muñoz et al. 2014).
The pan-sharpening capability of multi-temporal Landsat 8 imagery was used to increase the spatial resolution of the 30 m multispectral bands to 15m (Gilbertson et al. 2017). Moreover, using a thermal infrared instrument onboard the Landsat 8 can provide land surface temperature to detect burning areas.

2.2 The Hysplit

The Hysplit is the Air Resources Laboratory's' Hybrid Single-Particle Lagrangian Integrated Trajectory (HYSPLIT) model and a complete system for computing both simple air parcel trajectories and complex dispersion and deposition simulations (Stein et al. 2015). The model calculation method is a hybrid between the Lagrangian approach, which uses a moving frame of reference as the air parcels move from their initial location, and the Eulerian approach, which uses a fixed three-dimensional grid as a frame of reference(Draxler and Rolph 2010). By using this model, the emission trajectory of each point on the earth can be estimated.

3 RESULTS

3.1 Thermal anomalies identification

Based on VIIRS products on the World view map, 33 active thermal anomalies have been observed in 2017 and 2018. These active areas are shown in Figure 3. Furthermore, Table 1 indicates the number of days when these anomalies have activated. Peak time also illustrates the months these anomalies have detected mostly. The

observations show that the number of active burning days decreased in 2018.
According to Table 1, among the detected non-systematic emission sources, 4 areas are agricultural sources. Agricultural sources are most active in June and July. Besides agricultural lands, there is the Kahrizak municipality waste center which is known as the center of waste management system in Tehran. Thermal anomalies in this area show the municipal waste burning activity in which releases pollutants through burning. The number of days of thermal anomalies detected in this area has increased from 17 days in 2017 to 22 days in 2018.

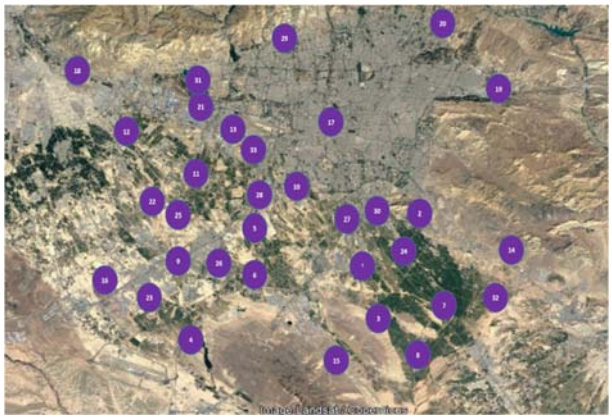

Figure 3 Thermal anomalies in Tehran and surrounding areas

Also, some emission sources are located very close to one another. For instance, there is a livestock facility beside a cement factory which is indicated by number 2 in Figure 3.

3.2. Landsat 8 satellite

After the identification of thermal anomalies caused by agricultural activities, Landsat 8 imagery was used to evaluate the accuracy of the assumptions.

Therefore, after evaluating the number of days in which the thermal anomalies were observed during a year, the Landsat 8 pictures were studied and after atmospherically corrected, a clear image of burning crops during these days was observed by the pan-sharpening algorithm.

Thermal bands were used for the identification of high-temperature points in the area. Four Landsat 8 level 1T images captured during 2017 and 2018 when agricultural thermal anomalies were active. Figure 4 and Figure 5 have shown the emissions of these areas.

Table 1 Thermal anomalies in Tehran and surrounding areas

	Peak time	2017	Peak time	2018
1	Jun/Oct	273	June/Sep	228
2	Jun/Oct	274	June/Aug	245
2	Jun/Oct	20	June/Aug	16
3	Jan/June	16	June	7
4	May	8		0
5	May/June	52	June/July	33
6	July/Aug	13	July	6
7	June/July	24	June	17
8	June	26	March	19
9	Feb	3	Aug	2
10	May/June	40	July	29
11	Feb/April	14	March	6
12	June/July	31	May/July	21
13	June	9	Sep/Oct	4
14	May/June/Aug	114	June/July	90
15	July/Sep	17	June/July	22
16	June/Sep	32	Jan/Aug	10
17	March	5	March	9
18	April/May	17	Aug	5
19	May/June	7	June/July	15
20	July	11	March	4
21	June	9	May	6
22	May	8	July	7
23	June/July	35	June	28
24	June/July	11	June	13
25	June/Aug	10	April	5
26	June	7	June	7
27	June	13	Oct	1
28	July	6	June/July	18
29	July	1	June	1
30	August	2	June	15
31	Nov	1	Sep	5
32	Nov	1	June/July	21
33	Nov	1	July	1

3.3. Hysplit model

Time and place of the thermal anomalies which are related to crop waste and municipal waste burnings areas were identified in 5 main points around Tehran. However, the emission effect of these areas on Tehran's air quality can be different based on the meteorological condition of places and the land topography. In this case, the Hysplit model is used for trajectory of emissions in the times that burnings mostly happened.

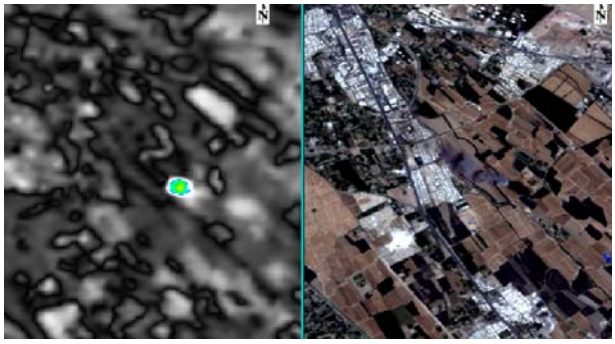

Figure 4 Burning wastes near the livestock plant

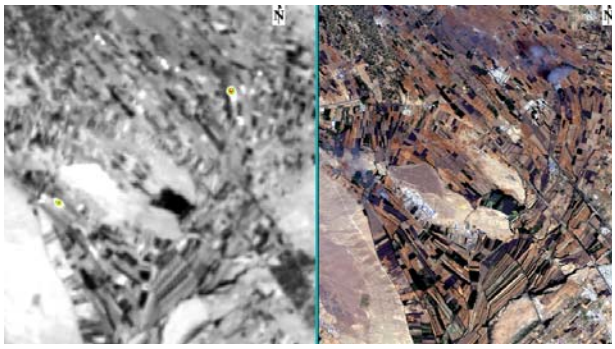

Figure 5 Burning crop in a sample agricultural land

Among the identified agricultural emission sources, emissions related to the livestock in Figure 6 paths from east of Tehran and do not affect the Tehran residential sector. Emissions from crop waste burning which is located in the south of Tehran in Figure 7 and Figure 8 passes from east to the center of the city, and therefore, may have a direct effect on Tehran's air quality.

Also, the burning emissions from the municipal waste management complex which is located in the south of the city pass through west to the center of Tehran (Figure 9). And finally, the emissions from the crop waste burning in the west of Tehran directly passes through the west of the city (Figure 10).

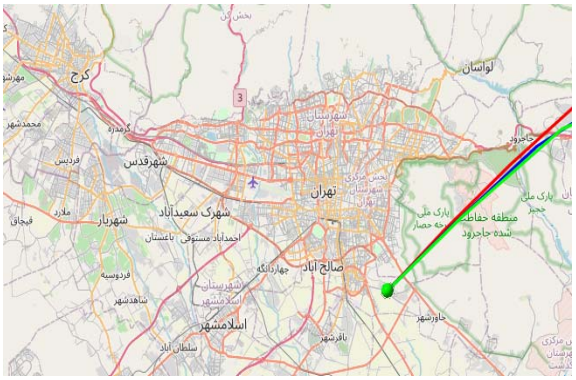

Figure 6 Trajectory of emissions from Livestock 8th June 2017 in the heights of 100,250 and 500m

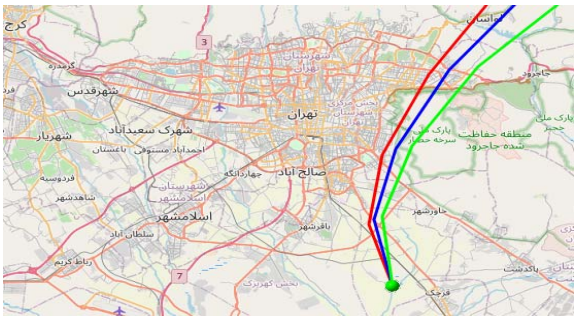

Figure 7 Trajectory of emissions from agricultural waste burning 8th July 2017 in the heights of 100,250 and 500m

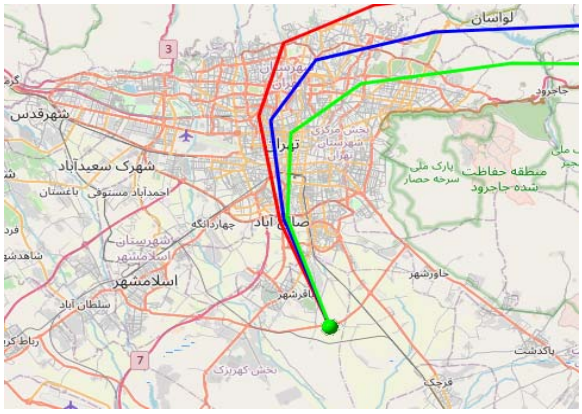

Figure 8 Trajectory of emissions from agricultural waste burning in 29th June 2017 in the heights of 100,250 and 500m

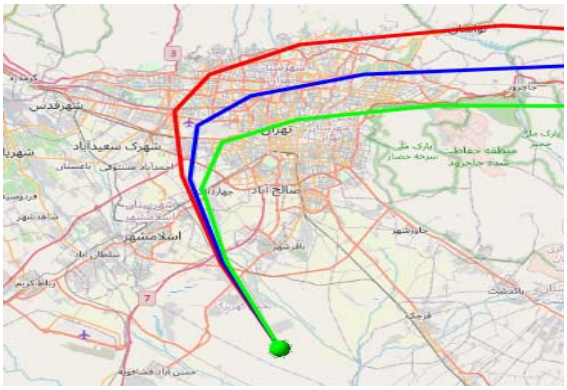

Figure 9 Trajectory of emissions from municipal wastes 29th June 2017 in the heights of 100,250 and 500m

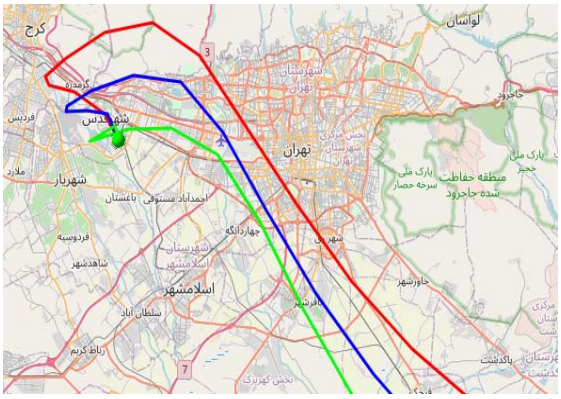

Figure 10 Trajectory of emissions from agricultural waste burning 29th June 2017 in the heights of 100,250 and 500m

4. DISCUSSION

Air pollution monitoring stations are distributed in different locations of the city to monitor the air quality of all residential districts of Tehran. Figure 11 shows the location of these stations. As most of the agricultural thermal anomalies occur in the south of the city, the Shahrerey air quality monitoring station which is located in the south of the city has been observed (circled in Figure 11). The hourly $PM_{2.5}$ concentrations in this station are evaluated in days in which all agricultural thermal anomalies were active (Figure 12). The recorded concentrations are then compared with the hourly concentrations during the following days when no agricultural waste burning happened (Figure 13).

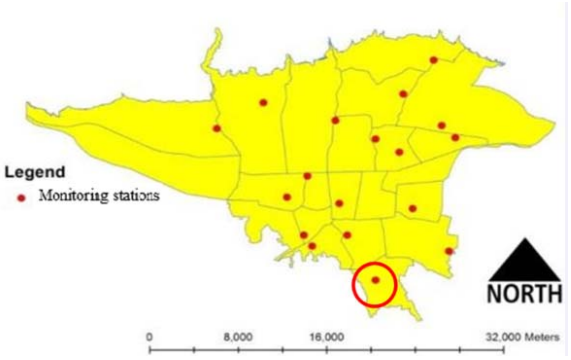

Figure 11 Tehran air pollution monitoring stations map

The concentrations of $PM_{2.5}$ in Figure 12 and 14 are monitored at the end of June when the burnings happen more than other months in 2017.

According to the measured concentration near the agricultural waste burning areas, it is shown that the $PM_{2.5}$ concentration increases slightly from 9 AM to 1 PM in the area. This might be due to the change of the agricultural waste burning activities in the studied period.

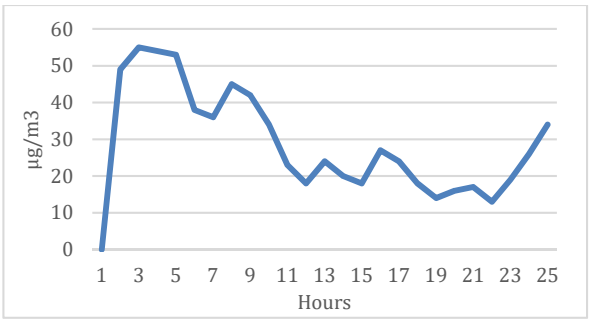

Figure 12 $PM_{2.5}$ concentration in the Shahrerey station with no agricultural active point in the area Date:06/30/2017

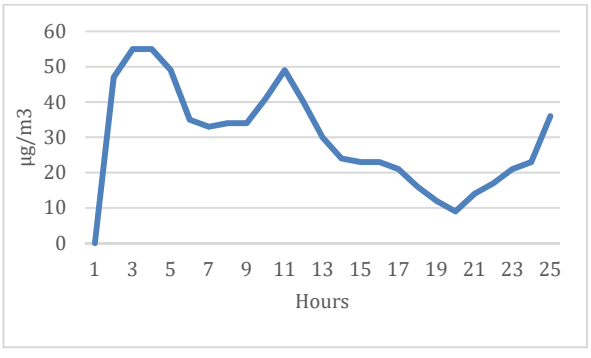

Figure 13 $PM_{2.5}$ concentration in the Shahrerey station 5 active agricultural point in the area Date: 06/28/2017

4. CONCLUSION

Crop residue burning and municipal waste burning must be accounted for among the air pollution sources in Tehran. In Tehran's emission inventory which has been gathered by AQCC, the agricultural waste burning and city waste burning has been neglected. However, other studies indicated that as high as 5% of total emissions in the city may be contributed from the agricultural sector.

Crop residue burning has occurred in 4 points in Tehran's surroundings. The agricultural waste burning, have happened in June and July more frequently. These months are considered less polluted in Tehran. Also, the number of days in which the anomalies have been observed in these areas decreased in 2018.

Besides agricultural waste burning areas, there is a municipal waste management complex near the city that shows thermal anomalies mostly in June and September in 2017. The number of times anomalies that are observed in this area increased in 2018.

The Hysplit model indicates that most of the emissions from thermal anomalies related to agricultural wastes and crop residue burning can affect Tehran's air quality as their emission trajectories path through Tehran and surroundings in the peak times of burnings. Consequently, the results of the research work suggest that agricultural waste burning is not neglectable and therefore, must be accounted for in the city emission inventory reports. Also, the promotion of cleaner waste management policies and measures is essential for air quality management in Tehran.

5. Reference

Csiszar, I., W. Schroeder, L. Giglio, E. Ellicott, K. P. Vadrevu, C. O. Justice, and B. Wind, 2014: Active fires from the Suomi NPP Visible Infrared Imaging Radiometer Suite: Product status and first evaluation results. Journal of Geophysical Research: Atmospheres, 119, 803-816.

Draxler, R., and G. Rolph, 2010: HYSPLIT (HYbrid Single-Particle Lagrangian Integrated Trajectory) model access via NOAA ARL READY website (http://ready. arl. noaa. gov/HYSPLIT. php). NOAA Air Resources Laboratory. Silver Spring, MD, 25.

Gilbertson, J. K., J. Kemp, and A. Van Niekerk, 2017: Effect of pan-sharpening multi-temporal Landsat 8 imagery for crop type differentiation using different classification techniques. Computers and Electronics in Agriculture, 134, 151-159.

Jiménez-Muñoz, J. C., J. A. Sobrino, D. Skoković, C. Mattar, and J. Cristóbal, 2014: Land surface temperature retrieval methods from Landsat-8 thermal infrared sensor data. IEEE Geoscience and remote sensing letters, 11, 1840-1843.

Martin, H., and S. Maria, 2018: Air Pollution in Tehran : Health Costs, Sources, and Policies. Environment and Natural Resources Global Practice Discussion Paper, World Bank.

Shahidzadeh, H., 2019: Tehran emission inventory

Singh, T., A. Biswal, S. Mor, K. Ravindra, V. Singh, and S. Mor, 2020: A high-resolution emission inventory of air pollutants from primary crop residue burning over Northern India based on VIIRS thermal anomalies. Environmental Pollution, 266, 115132.

Stein, A., R. R. Draxler, G. D. Rolph, B. J. Stunder, M. Cohen, and F. Ngan, 2015: NOAA's HYSPLIT atmospheric transport and dispersion modeling system. Bulletin of the American Meteorological Society, 96, 2059-2077.

Taksibi, F., H. Khajehpour, and Y. Saboohi, 2020: On the environmental effectiveness analysis of energy policies: A case study of air pollution in the megacity of Tehran. Science of The Total Environment, 705, 135824.

TAQCC, 2020: Tehran Annual Air and Noise Quality Report, period of March 2019-March 2020.

Vermote, E., C. Justice, M. Claverie, and B. Franch, 2016: Preliminary analysis of the performance of the Landsat 8/OLI land surface reflectance product. Remote Sensing of Environment, 185, 46-56.

VIIRS, 2020: https://viirsland.gsfc.nasa.gov/PDF/VIIRS_activefire_375m_ATBD.pdf.

WORLDVIEW: https://worldview.earthdata.nasa.gov/